

Charm ‘in’ the Photon

J. M. Butterworth

Department of Physics and Astronomy,



University College London, UK

ZEUS Collaboration

E-mail: jmb@hep.ucl.ac.uk

Abstract

Some recent ZEUS results on the photoproduction of open charm and possible implications for photon structure are discussed.

1 Open Charm Photoproduction at HERA

Photoproduction of ‘open’ charm (as opposed to $c\bar{c}$ bound states) can take place via several processes at HERA. The most obvious is photon-gluon fusion. The photon interacts directly with a gluon from the proton via t -channel charm quark, producing a high transverse energy charm balanced by an anticharm (Fig. 1a).

At high enough transverse energies, the c and \bar{c} will each lead to the formation of jets of hadrons. One hadron in each jet will in general be charmed. Photon-gluon fusion is often assumed to be the dominant, or indeed only, process.

Nevertheless, other possible production mechanisms exist. The photon can fluctuate into a $q\bar{q}$ state which may be long lived on the timescale of strong interactions. The $q\bar{q}$ state can thus form a complex partonic structure. Partons from the photon can then undergo hard scattering with partons from the proton - so called ‘Resolved Photon’ interactions. This allows the possibility of charm production via gluon-gluon fusion (Fig. 1b), where one gluon comes from the proton, the other from the photon.

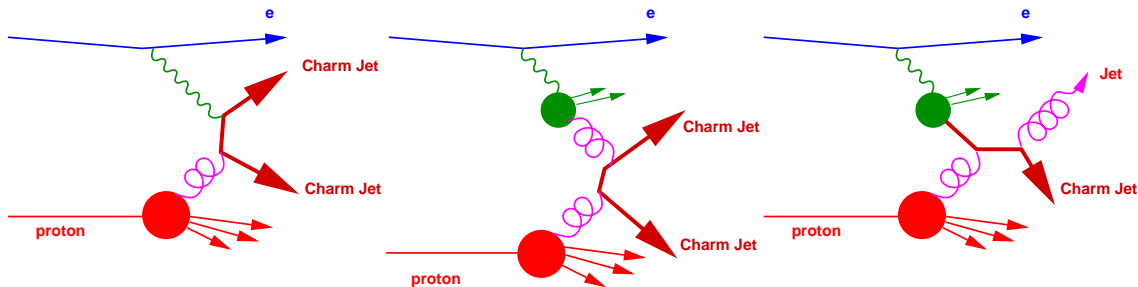


Figure 1: a) *Photon Gluon fusion* b) *Gluon Gluon fusion* c) *Charm excitation*.

This process is very similar to direct photoproduction, producing two high E_T^{Jet} jets each containing a charmed hadron. The difference is that only a fraction of the photon’s

momentum enters into the jet production, the rest being carried off in a photon remnant.

A further class of resolved processes can be imagined. What if the parton structure evolved by the photon contains charm? In this case, so-called ‘charm excitation’ processes can take place (Fig. 1c).

This process also leads to two high E_T^{Jet} jets, but only one of them contains a charmed hadron. The second charmed hadron is carried off in the photon remnant.

It is interesting to ask whether the resolved diagrams are important. The contribution of the first is especially sensitive to the gluon distribution inside the photon, whereas the second addresses the question as to whether charm is somehow generated ‘inside’ the photon.

We should ask how charm could be generated ‘in’ the photon. Might it happen via $\gamma \rightarrow c\bar{c}$ or $g \rightarrow c\bar{c}$? Is it perturbatively calculable? One has to be careful to define what exactly is meant by charm inside the photon. It is important to note that at NLO the division between ‘charm excitation’ and ‘boson gluon fusion’ (and indeed between resolved and direct photoproduction in general) will depend upon the choice of factorization scale. Moving factorization scale can turn a LO charm excitation diagram into a NLO direct photoproduction diagram, as illustrated in Fig. 2. A similar arbitrariness is present between charm generated via gluon splitting or assigned to the gluon-gluon fusion process.

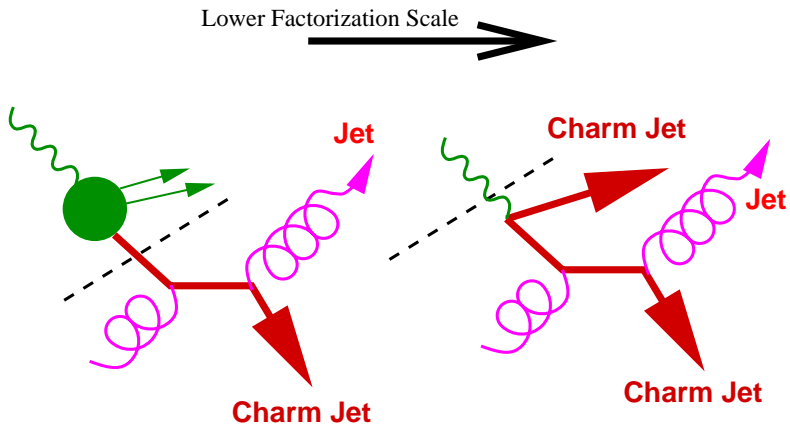


Figure 2: *NLO confusion*

Thus the discussion of any results will to some extent depend upon what approximations are used in the calculations to which the data is being compared.

1.1 Massless or Massive?

Currently two different approximations are used in the calculation of charm photoproduction at next-to-leading order.

- **Resummed, or ‘Massless’.** This approach uses $\mathcal{O}(\alpha_s^2)$ matrix elements for charm treated as a massless parton over the threshold for its production. Charm is an active flavour in the photon, present at a level dependent upon the choice of parton distribution set. By allowing charm to be generated in the evolution of the photon parton distribution, this approach resums logarithms of E_T^{Jet}/m_c [1, 2].

It is expected that this scheme will be a good approximation at $E_T^{\text{Jet}} \gg m_c$.

- **Massive.** In this approach, $\mathcal{O}(\alpha_s^2)$ matrix elements for massive charm are used. There is no charm content assigned to the parton distributions inside the photon. No resummation of E_T^{Jet}/m_c logarithms is performed [3].

It is expected that this scheme will be a good approximation when $E_T^{\text{Jet}} \approx m_c$.

In the jet measurements to be discussed below [4], $E_T^{\text{Jet}} \approx 7$ GeV.

1.2 Measuring Charm

The most commonly used method so far for tagging charm at HERA is the D^* tagging method [5]. This technique exploits the fact that the mass difference between the D^* and D^0 is small. Thus by cutting on this reconstructed mass difference as well as the mass, a relatively pure sample of charmed events is obtained.

2 Inclusive D^* Cross Section

A sample of charm events is selected using the following cuts;

- $p_T(D^*) > 2.0$ GeV, (when the D^0 decays to $K\pi$) or $p_T(D^*) > 4.0$ GeV, (when the D^0 decays to $K\pi\pi\pi$)
- $|\eta(D^*)| < 1.5$.
- $130 < W_{\gamma p} < 280$ GeV
- $Q^2 < 1$ GeV²

The differential cross section $d\sigma/dp_T(D^*)$ is shown in Fig. 3, compared to various NLO QCD calculations.

It can be seen that even with an extreme choice of parameters such as the charm mass, the massive scheme tends to lie below the data (dotted line). In addition, there is a significant discrepancy between the two groups using massless charm calculations.

The differential cross section $d\sigma/d\eta(D^*)$ is shown in Fig. 4.

Again, the massive calculations generally lie below the data, especially in forward direction, and the discrepancy between the two different massless calculations is clear. In the massless scheme, this cross section has a sensitivity to the parton distributions in the photon which is of the same order as the other uncertainties at present.

3 Photoproduction of Charm in Jets

Further information about the charm production mechanism can be obtained by measuring jets in high E_T^{Jet} photoproduction and looking for charm inside the jets. This has been done, again using the D^* tagging method, in a similar W range and with $E_T^{\text{Jet}} > 6$ GeV, $p_T(D^*) > 3$ GeV. The jets are defined using the K_T algorithm [6] in ‘inclusive’ mode [7].

Especially given the excess of data over the massive charm calculations, it is of course interesting to separate direct and resolved samples. This is possible using the variable [8]:

$$x_\gamma^{\text{OBS}} = \frac{\sum_{\text{jets}}(E_T^{\text{Jet}} e^{-\eta^{\text{jet}}})}{2E_e y}$$

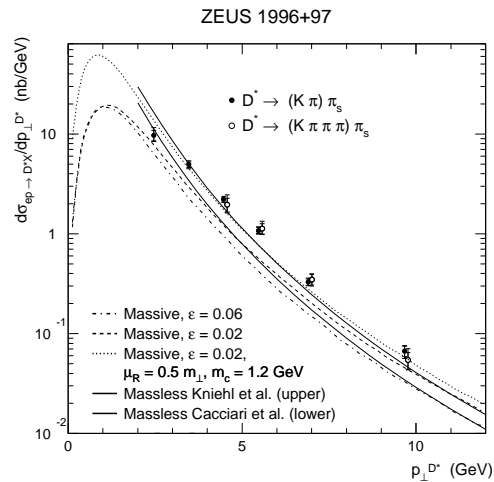


Figure 3: $d\sigma/dp_T(D^*)$ The MRSG [9] and GRV-G HO [10] parton density functions are used for the proton and the photon respectively.

ZEUS 1996+97

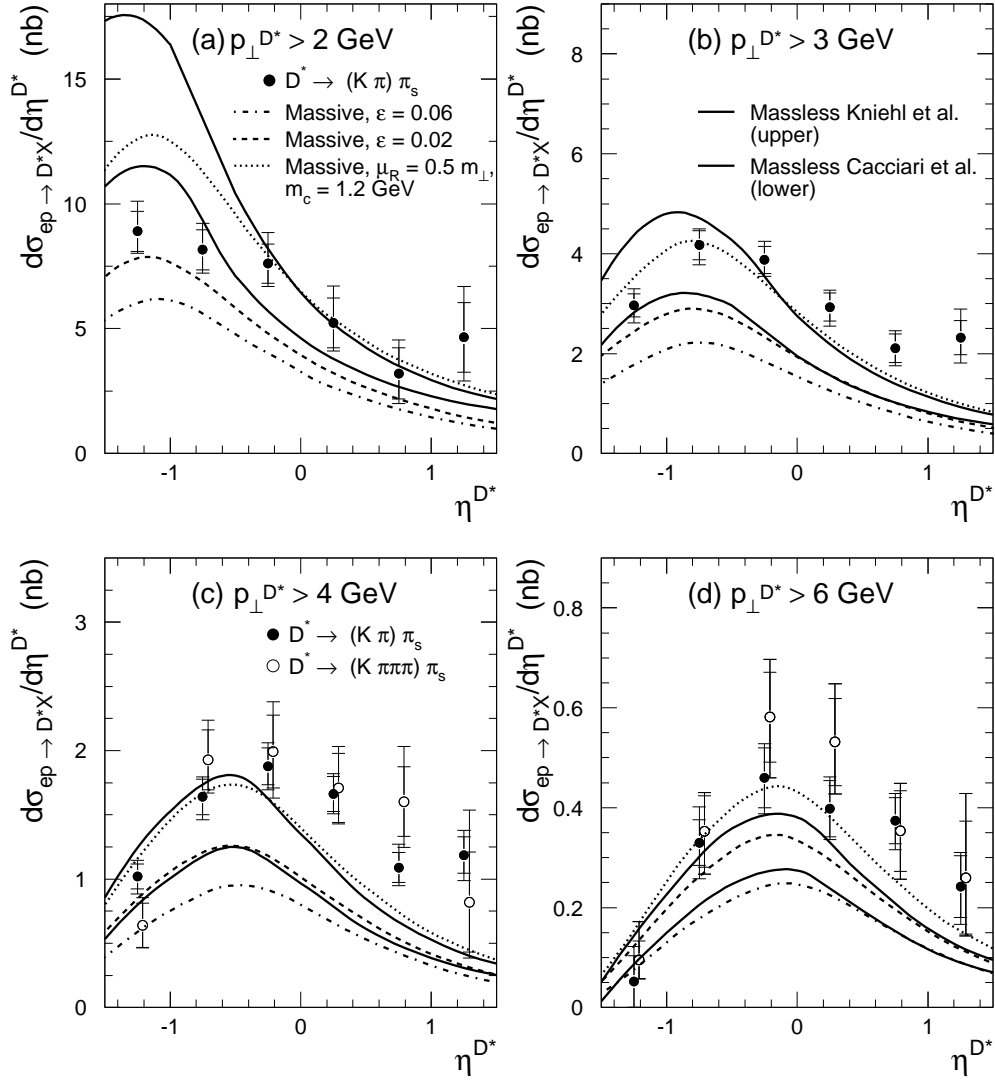


Figure 4: $d\sigma/d\eta(D^*)$ The MRSB [9] and GRV-G HO [10] parton density functions are used for the proton and the photon respectively.

which is the fraction of the photon's momentum which participates in the production of the two highest E_T^{Jet} jets. Thus LO direct process have $x_\gamma^{\text{OBS}} = 1$ and LO resolved processes have lower x_γ^{OBS} , although x_γ^{OBS} itself is of course defined independently of the order of the calculation.

Fig. 5 shows the energy flow around jets, compared to the expectation from the HERWIG Monte Carlo. The energy flow in the rear (negative $\Delta\eta$) region shows evidence for presence of a photon remnant in a significant fraction of the events at low x_γ^{OBS} .

The cross section $d\sigma/dx_\gamma^{\text{OBS}}$ is shown in Fig. 6. The cross section at lower x_γ^{OBS} values is significant, indicating that LO direct processes alone cannot describe charm production successfully. In particular, the data is inconsistent with the LO Direct process in HERWIG shown in the figure, even after the effects of parton showering and hadronisation are included in the Monte Carlo. Such effects can populate the low x_γ^{OBS} region even with direct events, but do not do so sufficiently. In fact the data

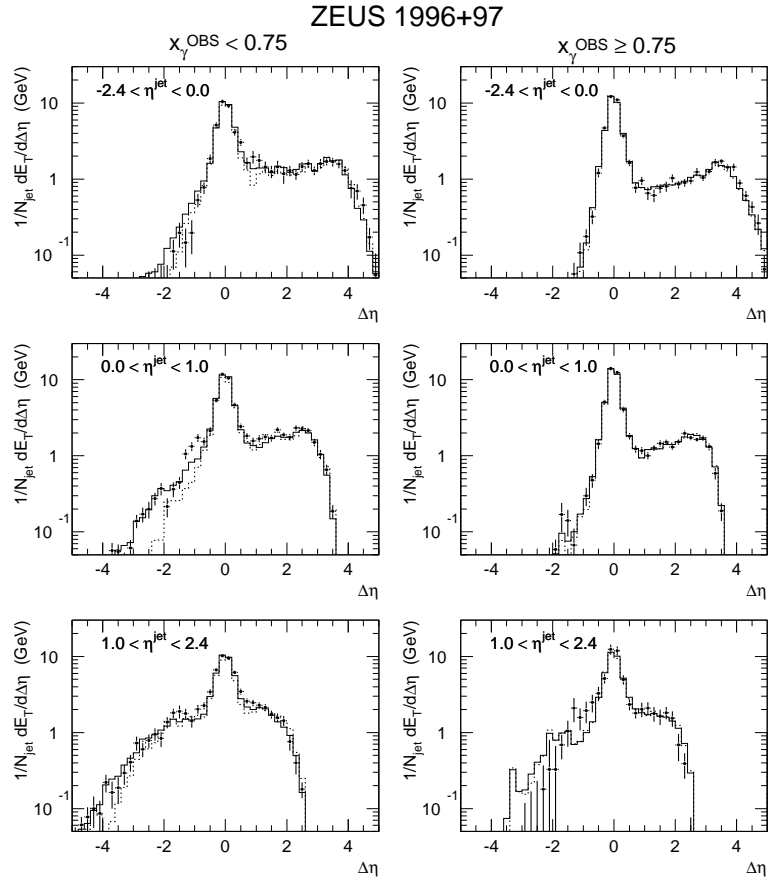


Figure 5: *Energy flow around jets*

require a $(45 \pm 5)\%$ LO resolved contribution from HERWIG.

Furthermore, according to HERWIG this resolved contribution is almost entirely charm excitation.

Also shown, in the lower half of Fig. 6, is a NLO massive calculation of $d\sigma/dx_\gamma^{\text{OBS}}$. The calculation lies below the data at low x_γ^{OBS} . It should be remembered that hadronisation is not included in the NLO calculation and this may affect the comparison. Nevertheless, the data suggest a larger resolved contribution than is present in the calculation.

4 Summary

A significant cross section for the ‘resolved’ photoproduction of charm has been measured. The theory is ‘close but no cigar’ in inclusive D^* and charmed jet measurements, lying in general somewhat below the data particularly in the forward and low- x_γ^{OBS} regions.

Comparison to the HERWIG simulation, which includes LO matrix elements, leading logarithmic parton shower and a hadronisation model, requires a charm excitation contribution of about 45% in the kinematic regime measured here.

The parton distribution functions used in the theory comparisons do not always represent the state-of-the-art in their massive quark treatment, and our understanding should benefit from a comparison to other parameterisations.

The data represent a challenge to the theory to truly understand charm production ‘inside’ the photon. This challenge is likely to get tougher as more accurate measurements over wider kinematic regimes become possible from both H1 and ZEUS with micro-vertex detectors, the introduction of other tagging methods, and higher luminosity from the coming HERA upgrade. I would like to acknowledge the enormous efforts of the ZEUS heavy flavour group, as well as the theory groups who provided the calculations, many of whom will undoubtedly be responsible for these coming advances.

References

- [1] M.Cacciari et al., Phys. Rev. D55 (1997) 2736; *ibid* 7134;
M.Cacciari, private communication.
- [2] B.A.Kniehl et al., Z. Phys. C76 (1997) 689;
J.Binnewies et al., Phys.Rev.D58 (1998) 014014.
Phys. Rev. D (1998) in print;
B.A.Kniehl, private communication.
J.Binnewies et al., Z. Phys. C76 (1997) 677.
- [3] S. Frixione et al. Nucl. Phys. B 412 (1994) 225.
- [4] ZEUS Collaboration, J. Breitweg et al, DESY 98-085, to appear in Eur. Phys. J. (1998 in print).
- [5] S. Nussinov, Phys. Rev. Lett. 35 (1975) 1672;
G.J. Feldman et al., Phys. Rev. Lett. 38 (1977) 1313.
- [6] S.Catani et al., Nucl. Phys. B 406 (1993) 187.
- [7] S.D.Ellis and D.E.Soper, Phys. Rev. D 48 (1993) 3160.
- [8] ZEUS Collaboration, M. Derrick et al, Phys. Lett. B348 (1995) 665.
- [9] A.D. Martin, W.J. Stirling and R.G. Roberts, Phys. Lett. B 354 (1995) 155.
- [10] M. Glück, E. Reya and A. Vogt, Phys. Rev. D 46 (1992) 1973.

ZEUS 1996+97

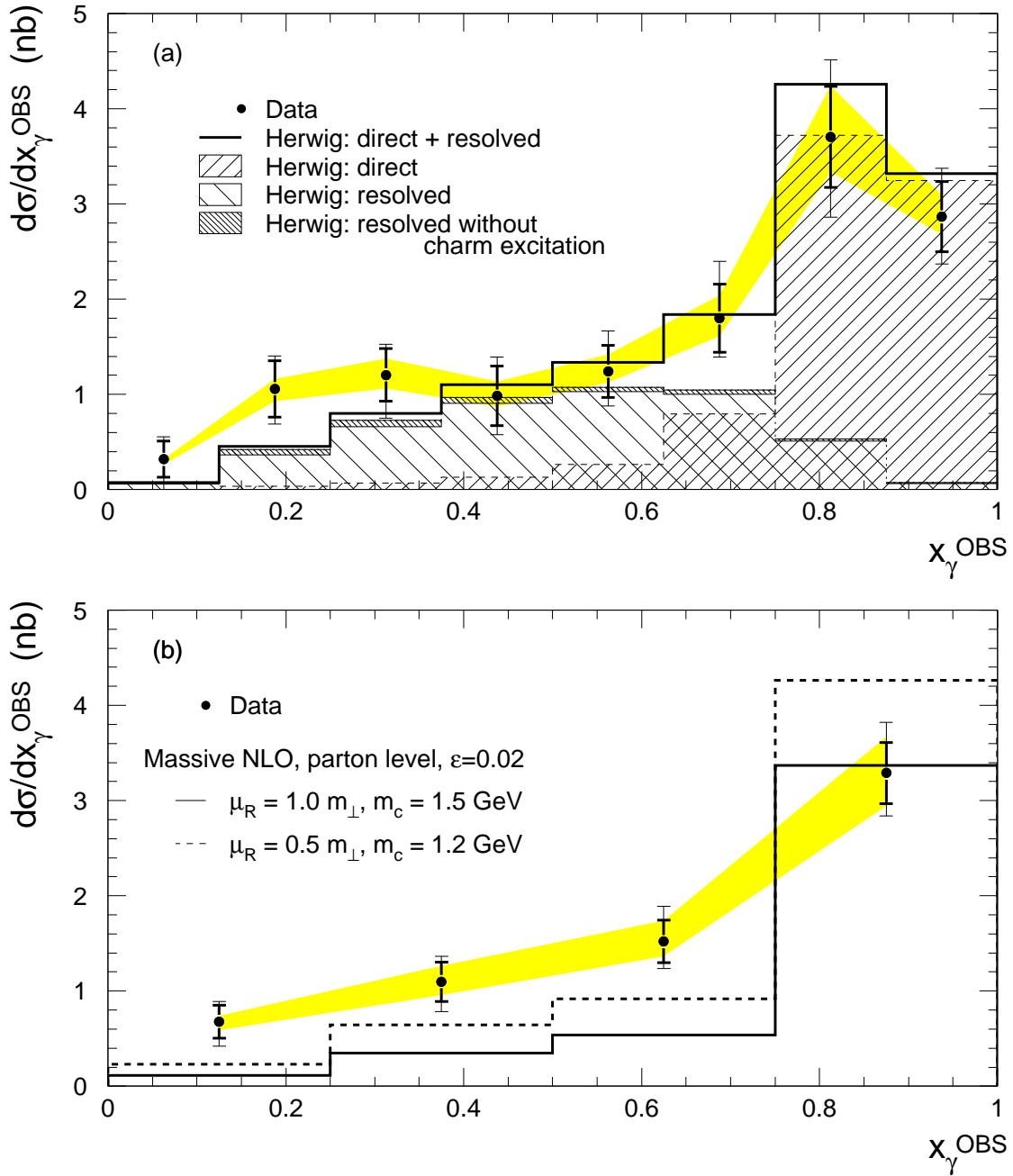


Figure 6: $d\sigma/dx_\gamma^{\text{OBS}}$ The MRSG [9] and GRV-G HO [10] parton density functions are used for the proton and the photon respectively.